Microscopic acid–base equilibria of a synthetic hydroxamate siderophore analog, piperazine-1,4-bis(*N*-methylacetohydroxamic acid)

M. Amélia Santos,[a] M. Alexandra Esteves,[a] M. Cândida Vaz,[a] J. J. R. Fraústo da Silva,[a] Bela Noszal[b] and Etelka Farkas[c]

[a] *Centro de Química Estrutural, Complexo 1, Instituto Superior Técnico, 1096 Lisboa-codex, Portugal*
[b] *Semmelweis Medical University, Budapest, Hungary*
[c] *L. Kossuth University, Debrecen, Hungary*

The protonation behavior of the cyclic diaminodihydroxamate ligand, piperazine-1,4-bis(*N*-methylacetohydroxamic acid) (H_2L^1), has been studied at both the macroscopic and the microscopic level. Potentiometric and ^{1}H NMR techniques have been used for the study of this ligand as well as several model compounds: *N*-methylchloroacetohydroxamic acid, glycinehydroxamic acid and piperidino(*N*-methylacetohydroxamic acid). Molecular modeling calculations have also been performed to predict the most stable conformations and to estimate relevant contributions to the overall protonation process.

The results of the protonation microconstants show that the *N*-donors in H_2L^1 are much less basic than the *O*-donors. The protonated amine moieties release most of their protons in the acid region while the deprotonation of the hydroxamate moieties starts only above pH 5. The theoretical modeling calculations show the effect of electrostatic interactions and internal hydrogen bonds on the interactivity of the basic sites throughout the protonation process.

Introduction

Siderophores are a class of naturally occurring iron-chelating compounds which are produced by microorganisms to transport iron from the environment into cells. The development of siderophore analogs has been the object of much interest, given their potential use as pharmaceutical drugs, in particular for chelation therapy.[1,2]

We have been involved recently in the study of polyazapolyhydroxamate ligands as analogs of siderophores.[3,4] The ligand piperazine-1,4-bis(*N*-methylacetohydroxamic acid) (H_2L^1)[5,6] is one example of this new family of biomimetic binders which has been proven to be a reasonable model of rhodotorulic acid, a naturally occurring dihydroxamate siderophore produced by *rhodotorula pilimane*.[7] This siderophore analog has four protonation sites (two hydroxamate and two amino groups) and thus, depending on pH, H_2L^1 can exist in solution as a variety of protonated species. The corresponding protonation macroconstants were determined by potentiometry in a previous work.[5] However, macroconstants only give quantitative information about the basicity of proton-binding sites when protonation occurs independently. The fact that this ligand has some protonation sites of similar basicity indicates that overlapping of protonation processes may occur and so, for a certain pH, it is possible to have protonation isomers presenting quite different properties in terms of metal ion coordination and corresponding biological processes.

Therefore, since the protonation macroconstants calculated for H_2L^1 do not characterize sufficiently the acid–base behavior of the individual proton binding sites of this ligand,[8,9] its protonation process has been studied further. The present paper reports the results obtained.

It is well known that the protonation of a basic site leads to electronic deshielding effects on the adjacent methylene (or methyl) protons, the magnitude of such effects being dependent on the type of basic center.[10] The average chemical shift of the nearby carbon-bonded protons, as a function of pH, is expected to reflect the fractional protonation of each basic group. Thus, these studies afford a qualitative picture of the protonation sequence. Furthermore, they enable the calculation of parameters characterizing the acid–base properties, which can be used for the construction of the complete protonation scheme of this molecule and determination of the protonation microconstants, as well as the corresponding microspeciation.

Thus, to obtain further insight into the protonation sequence for H_2L^1, ^{1}H NMR titrations were carried out for this ligand as well as for several model compounds: *N*-methylchloroacetohydroxamic acid (HL^2), glycinehydroxamic acid (HL^3) and piperidino(*N*-methylacetohydroxamic acid) (HL^4). The model compounds are simpler derivatives of the parent ligand and proved to be useful in establishing the individual basicity and NMR–pH profile of each proton binding site.[8]

Molecular modeling calculations were also performed on the neutral and protonated forms of H_2L^1, HL^4 and some related species, to help the understanding of the protonation behavior at both the macroscopic and the microscopic level.

Results

The stepwise protonation constants for H_2L^1 and related model ligands, calculated from data of potentiometric titrations ($T = 25.0 \pm 0.1$ °C; $I = 0.1$ M KNO_3) or obtained from the literature, are summarized in Table 1. H_2L^1 has a cyclic diamine

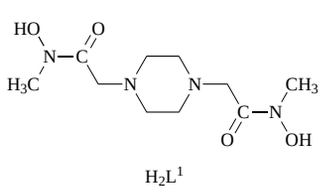

H_2L^1

moiety (piperazine) connecting two hydroxamic acid arms. Data for the model compounds, reported in Table 1, show that the basicity of piperazine (L^5) nitrogens (log $K_1 = 9.84$; log

Table 1 Stepwise protonation macroconstants for H_2L^1, HL^4, L^5, HL^2 and HL^3

Compound	log K_1	log K_2	log K_3	log K_4
$H_2L^{1\,a}$	9.53(2)	8.45(2)	6.67(2)	2.44(6)
$HL^{4\,b}$	9.79(1)	7.44(1)		
$L^{5\,c}$	9.84(2)	5.65(1)		
$HL^{2\,b}$	7.98(1)			
$HL^{3\,d}$	9.12(6)	7.37(3)		

[a] From ref. 5. [b] This work. [c] From ref. 11. [d] From ref. 12.

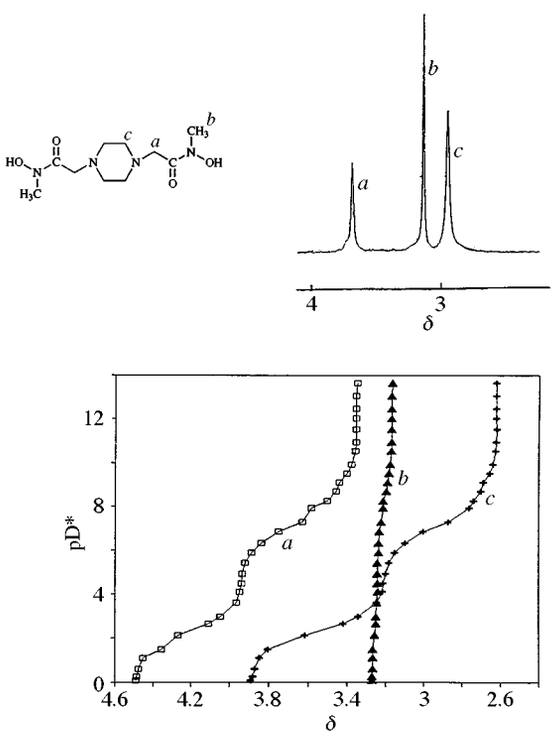

Fig. 1 ^{1}H NMR spectrum of H_2L^1 at pD* 7.0 and titration curves, δ as a function of pD* ($C_L = 2 \times 10^{-2}$ mol dm^{-3})

$K_2 = 5.65$)[11] is not too different from that expected for the hydroxamate groups (log K = 8–9).[12] So, a series of interactions may occur when H_2L^1 is protonated without the calculated macroconstants reflecting what happens at the level of each individual protonation site.

To obtain further information on the protonation sequence of H_2L^1, we have performed a ^{1}H NMR titration of this ligand; the set of curves obtained (Fig. 1) confirms that the protonation of each basic group produces an electronic deshielding effect on the nearby methylene (or methyl) protons with concomitant downfield shifts of the corresponding resonance peaks. The quantitative evaluation of this effect can be achieved using the so-called Sudmeier and Reilley[13] approach in which it is assumed that, associated to each methylene proton (i) adjacent to a basic center (j) being protonated, a mean protonation shift constant or shielding constant (C_{ij}) can be calculated; on the other hand, the contributions from the protonation of several different basic sites, in the vicinity of the methylene group, are additive and so $\Delta\delta = \Sigma_{i=1}^{n} C_{ij} f_j$, where f_j is the percentage of protonation. These C_{ij} values depend on several factors such as the type of basic center and the distance between the methylene group and the basic center considered. For a series of linear polyaminocarboxylates, Sudmeier and Reilley measured the shielding constants for methylene groups in the following moieties: CH_2COO^- (C_O = 0.20 ppm), CH_2NR_2 (C_{N_α} = 0.75 ppm) and $CH_2CH_2NR_2$ (C_{N_β} = 0.35 ppm). However, more recent studies[8,14] demonstrated that these values did not show self-consistency in the interpretation of the protonation of cyclic polyaminopolycarboxylates and appropriate cyclic

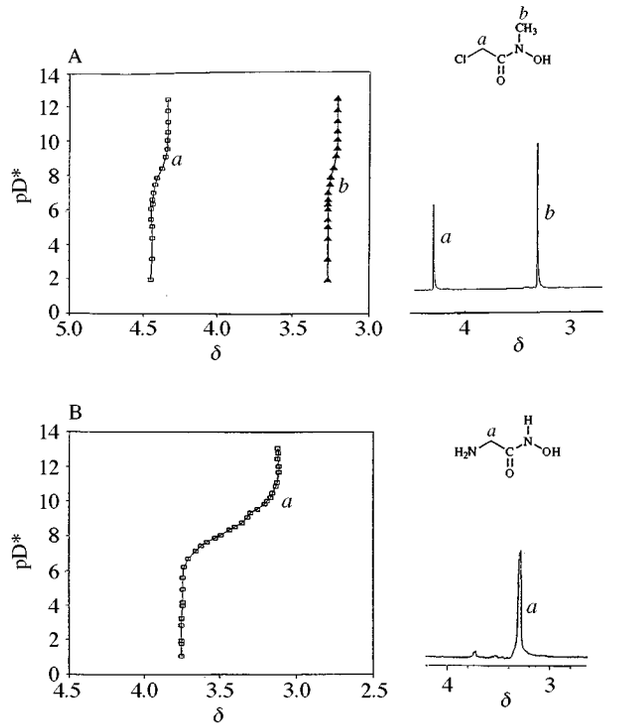

Fig. 2 ^{1}H NMR spectrum and titration curves (δ as a function of pD*), obtained for the ligands (A) HL^2 and (B) HL^3 ($C_L = 2 \times 10^{-2}$ mol dm^{-3})

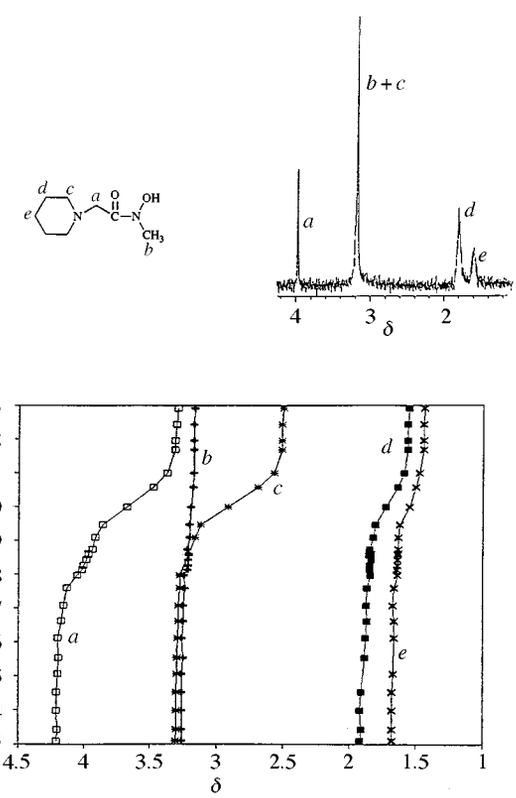

Fig. 3 ^{1}H NMR spectrum of HL^4 at pD* 8.2 and corresponding titration curves, δ as a function of pD* ($C_L = 2 \times 10^{-2}$ mol dm^{-3})

models had to be chosen which give slightly different values for the C_N shielding constants.

Although Sudmeiers shielding constants could be used for qualitative interpretation of the protonation sequence, suitable models were also used for quantitative determination of constants in the present work. Therefore, ^{1}H NMR titrations were also performed for the following model compounds: HL^2, HL^3 (Fig. 2) and HL^4 (Fig. 3). Table 2 summarizes all the chemical shifts calculated for the ligands.

Table 2 Chemical shifts ($\Delta\delta$) due to stepwise protonation of the amine (Δ^{N}) and hydroxamate (Δ^{H}) *n* basic sites, roughly evaluated for several atom types from the ^{1}H NMR titration

			$\Delta\delta$					
Molecule	Proton type	*n*	Δ^{H}_{a}	Δ^{N}_{a}	Δ^{N}_{b}	$\Delta^{N}_{c_\alpha}$	$\Delta^{N}_{c_\beta}$	$\Delta^{N}_{c_\gamma}$
HL^{2}	*a*, *b*	1	0.12	—	0.08	—	—	—
HL^{3}	*a*	1	0.64		—	—	—	—
		2						
HL^{4}	*a*, *b*, *c*	1	—	0.66	—	0.70	0.28	0.19
		2	0.22	—	0.09	—	—	—
H_2L^{1}	*a*, *b*, *c*	1	0.77		0.10	0.73	—	—
		2						
		3						
		4	—	0.68	—	0.88	—	—

Titration curves of HL^{2} [Fig. 2A] show the effect of hydroxamate protonation on methylene (*a*) and *N*-methyl type (*b*) protons. As expected, there is only one inflexion, which is equivalent to that obtained by potentiometric titration.

The ^{1}H NMR titration curve of HL^{3} [Fig. 2B] exhibits one main inflexion ($\Delta\delta = 0.64$) in the entire pD* range encompassing both the amine and hydroxamate protonations, thus suggesting that these processes are overlapping. Comparison of the inflexion magnitudes of HL^{2} and HL^{3} (Fig. 2A and B), clearly indicates that the deshielding effect produced in this *a* methylene proton by the *N*-amine protonation (Δ^{N}_{a}) is much higher than that of the hydroxamate protonation (Δ^{H}_{a}). A more detailed analysis of the HL^{3} *a* proton curve also reveals the existence of an apparently minor discontinuity at the first stage of the protonation process that can be taken as indicative of a slightly higher acidity of the NH_3^+ group relative to the NHOH group. Furthermore, protonation microconstants calculated for α-alaninehydroxamic acid from ^{13}C NMR experimental data[15] support that acidity order.

Unfortunately, the use of HL^{3} as a model to estimate the amine-protonation shift on the H_2L^{1} methylene *a* protons is limited due to the different substituents on the hydroxamate nitrogen in these compounds. Therefore, another model (HL^{4}, Fig. 3) has been selected, to improve the evaluation of the shielding effects on each non-labile proton.

The ^{1}H NMR spectrum of HL^{4} and the corresponding pH (pD*) dependent chemical shifts are shown in Fig. 3. The curves corresponding to the *a*, *c*, *d* and *e* protons exhibit well-defined inflexions centered at *ca.* pD* 10, while those for both the *a* and *b* protons present a small inflexion around pD* 8. Thus, this set of titration curves clearly shows that for this molecule the protonation of the hydroxamate group mostly occurs after the protonation of the amine group. It also gives an indication of the average chemical shifts produced by amine and hydroxamate protonation on each type of nearby non-labile protons. In effect, Table 2 shows that the amine protonation produces a deshielding effect on the *a* methylene protons ($\Delta\delta = 0.66$) which is about three to five times the effect of the hydroxamate protonation. Thus, the chemical shift induced in this methylene group provides useful information to help elucidate the sequence of protonation. Although the chemical shift produced in the *N*-methyl protons by the hydroxamate protonation is smaller than that involved in the methylene protons, it can still be used as a good probe for the protonation of this group. Table 2 shows the average chemical shift produced by the amine protonation on the cyclic methylene *c* protons which are α-, β- and γ-positioned relative to the amine group. The c_α methylene protons present an average chemical shift ($\Delta\delta = 0.70$) close to those of the *a* protons. As the number of bonds between the basic amino site and non-labile proton increases, the shift decreases dramatically ($\Delta\delta_\beta/\Delta\delta_\alpha = 40\%$; $\Delta\delta_\gamma/\Delta\delta_\alpha \approx 27\%$). The chemical shifts calculated for the c_α and c_β methylene protons ($\Delta\delta^{N}_{c_\alpha} = 0.70$ and $\Delta\delta^{N}_{c_\beta} = 0.28$) are comparable to the shielding constants referred to above, calculated by Sudmeier and Reilley,[13] for amine protonation of linear polyaminocarboxylates.

Therefore, based on results of model compounds, a general picture can be constructed for the protonation of H_2L^{1}: while the last protonation stage, corresponding to the inflexion of the *c* proton curve at *ca.* pD* 2, can be clearly attributed to protonation of an amine group ($\log K_4 = 2.44$), the protonation of the other three sites are not independent processes. A detailed analysis of the titration curves corresponding to *b* and *a* protons shows the existence of small inflexions around pD* 8, suggesting that, despite the interactivity in these protonation processes, the first stage of the protonation mostly involves a hydroxamate site.

Interactions of the protonation processes are also indicated by the small inflexion observed in the *b* proton curve at *ca.* pD* 2. This may be due to some disruption of hydrogen bonds involving the nitrogen atoms of amino groups and the nearby hydroxamate hydroxylic protons in a six-membered ring intermediate (see below for the diprotonated species).

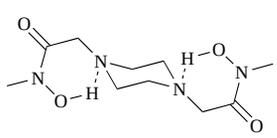

Such an effect could explain the fact that the ammonium protons of this ligand are more acidic than those in the corresponding cyclic amine (see Table 1), although the inductive effect of the hydroxamate groups should also be considered. The very easy dissociation of the first proton from the fully protonated ligand species can also be explained in terms of coulombic repulsive effects between the positive sites of the *N*,*N*-diprotonated species.

Providing an approximate qualitative characterization of the protonation sequence of H_2L^{1} is available, its quantitative evaluation is also possible using the Studmeier and Reilley approach, as has been carried out previously for the aminocarboxylic analog.[10] However, that method is limited, and is very dependent on the pH and the adequacy of the shielding constants used.[14]

For comparison, we have simulated the structure of some neutral and protonated species and tried to relate their relative stability and charge distribution to the microprotonation process. We began by modeling the neutral species of the aminohydroxamic acids HL^{4} and H_2L^{1}, with the hydroxamate moieties protonated. Both the global minima have the cyclic ring in a chair conformation and the hydroxamic acid 'arms' in equatorial positions. Fig. 4 shows the optimized geometries for all the models studied. The effect of different hydrogen bonding schemes on the heat of formation was first analysed for the monohydroxamate model HL^{4}. It was shown that stabilizing effects which could result from internal NOH···O=C hydrogen bonding (five-membered ring intermediate), expected

Table 3 Heats of formation ($\Delta_f H$), steric energy (E), Mulliken charges and H-bond length or H-contact distances (O···H or N···H) calculated for several species related to H_2L^1 and HL^4

Compound[a]	$\Delta_f H$/kcal mol^{-1} (AM1)	E/kcal mol^{-1} (MM/AM1)	Mulliken charges (AM1)				Distance/Å (AM1)	
			O	N	N′	O′	N···HO ($N^+H\cdots O$)	N′···HO′ ($N'^+H\cdots O$)
$[L^1]^{2-}$	−63.19	116.99	−0.698	−0.225	−0.266	−0.709	—	—
$[H_2L^1_{OO'}]$	−66.22	38.36	−0.247	−0.259	−0.254	−0.246	2.73	2.79
$[H_3L^1_{ONO'}]^+$	85.30	43.95	−0.246	−0.286	0.004	−0.289	(4.00	(2.24)
$[H_4L^1_{ONN'O'}]^{2+}$	320.49	80.23	−0.281	−0.003	−0.001	−0.312	(2.18)	(2.25)
L^5	−4.41[b]	27.07	—	−0.275	—	—	—	—
$[L^4]^-$	−59.61	42.97	−0.684	−0.233	—	—	—	—
$[HL^4_O]$	−52.07	29.18	−0.245	−0.265	—	—	2.67	—
$[H_2L^4_{ON}]^+$	96.79	40.65	−0.290	+0.006	—	—	(2.31)	—
L^6	−19.02	12.26	—	−0.298	—	—	—	—
L^7	−31.10[b]	17.42	—	−0.269	—	—	—	—
HL^8	−80.90	15.98	−0.243	—	—	—	—	—

[a] $[H_nL^i_{X\ldots Z}]^p$ means an n-protonated species of the ligand L^i, the n protons being localized on the n following atoms. [b] Geometry is not at stationary point.

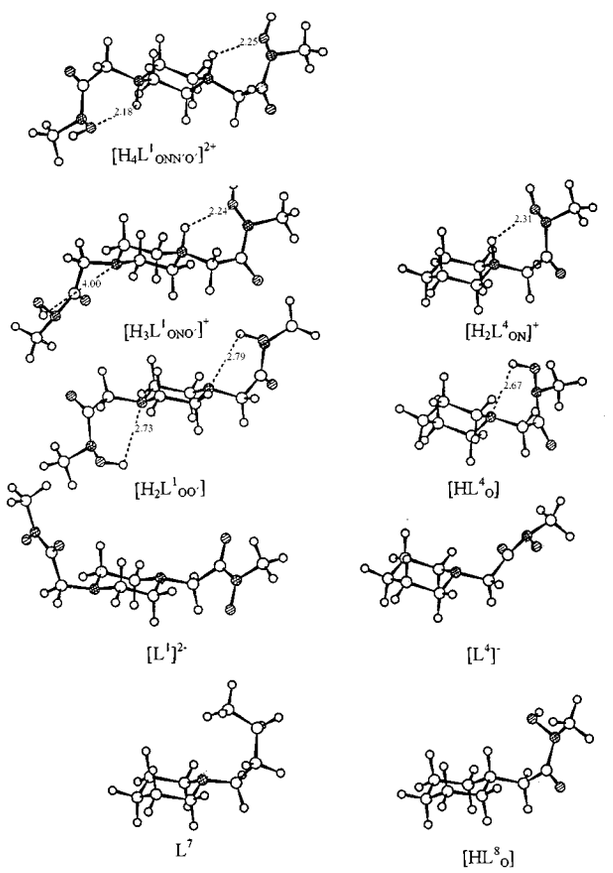

Fig. 4 Stereoviews of global minimum energy structures calculated for several species of H_2L^1, HL^4 and related model molecules, by the AM1 method. *O*-Atoms are shaded, and *N*-atoms are double shaded. H-Bond (or H-bond type contacts) are shown as dotted lines. The designation $[H_nL^i_{X\ldots Z}]^p$ means an *n*-protonated species of the ligand L^i, the *n* protons being localized on the *n* atoms X and Z.

for the *Z* form (*cis*) of the hydroxamate moiety,[16] are overcome by the effect of another hydrogen bonding interaction NOH···N, having a less constrained six-membered ring structure (involving the hydroxamate proton and the amine nitrogen atom), and also by the dipole–dipole stabilizing effects inherent in the adopted hydroxamate *E* form (*trans*).

Similarly, modeling the neutral diaminodihydroxamic acid (H_2L^1) leads to the global minimum energy conformation having the hydroxamate moieties in *E* (*trans*) conformation, thus leaving the hydroxamate protons free for interaction with the amine-nitrogen atoms, *via* hydrogen-bonded six-membered ring structures, tilted 'upward' or 'downward' from the chair ring of the backbone molecule. However, the calculated hydrogen bond lengths for HL^4 ($d^{H}_{N\cdots HO}$ = 2.67 Å) and hydrogen bond contacts for H_2L^1 ($d^{H}_{N\cdots HO}$ = 2.73, 2.79 Å) may be overestimated by the AM1 method.[17] The fact that larger distances have been obtained for the diaminodihydroxamate ligand should be attributed to coulombic repulsions between the concomitant positive-induced *N*-dipoles. So, it became apparent that the existence of one of the hydrogen bonding interactions prevents the formation of the second one. This model supports the existence of interactivity in the protonation process.

Although there are limitations to the application of semi-empirical methods to charged species,[18] we have also simulated the *N*-protonated species of HL^4 and H_2L^1. As expected, due to electrostatic effects, a strong interaction between the ammonium proton and the hydroxamate oxygen atom ($d_{NH\cdots OH}$ = 2.24 Å, H_2L^1) was observed. The large increase in energy associated with the second *N*-protonation, as compared with the first one, derives from the contribution of electrostatic terms. It gives support to the low value found for the last *N*-protonation constant for this diazadihydroxamate compound.

On the other hand, analysis of the AM1 Mulliken charges, calculated for the global minimum energy conformations corresponding to neutral species of HL^4 and H_2L^1 (see Table 3), shows that the charge on the amine-nitrogen atoms is more negative in the mono-amine (−0.265) than in the corresponding diamine compound (−0.256), thus supporting an easier *N*-protonation of the former compound when compared with the latter one. Similar charge differences were found for the corresponding unsubstituted cyclic amines [piperazine (L^5), piperidine (L^6)], which are also in agreement with differences in the corresponding basicities (log K^1 = 9.84 for L^5; log K^1 = 11.01 for L^6).[11]

Regarding the charges on the hydroxamate oxygens, it was shown that the corresponding anions have a higher charge in the dihydroxamate (−0.704) than in the monohydroxamate compound (−0.684). These differences may also be related to differences in the corresponding basicities. Finally, comparison of the charge distribution on the monoaminohydroxamic acid (HL^4) with the distribution calculated for related models [*N*-butylpiperidine (L^7) and *N*-methylcyclohexanylacetohydroxamic acid (HL^8)] suggests that the electron-withdrawing effect produced by the hydroxamate moiety on the amine group is more relevant than the corresponding reverse effect (see Table 1).

This molecular modeling approach allowed, therefore, a comparison of the preferred conformations and the acid–base behavior of the diaminodihydroxamate ligand (H_2L^1) and related models. It was shown that this cyclic α-amino-hydroxamic acid should have the cyclic diamine backbone in a chair conformation and the hydroxamate moieties of

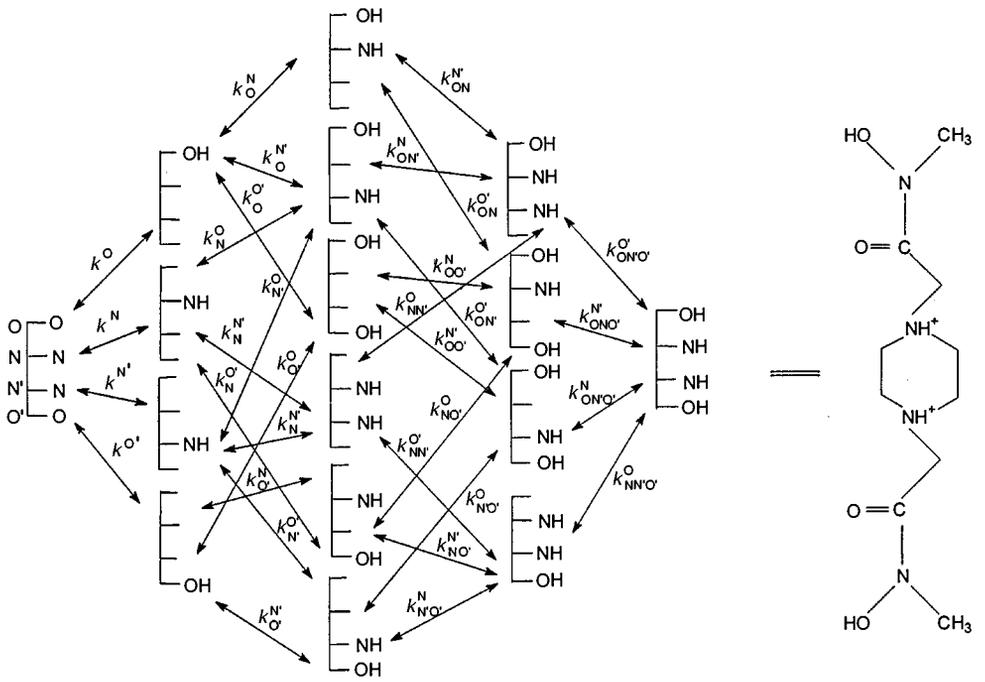

Scheme 1 Protonation scheme of H_2L^1

the side chain interacting with the nearby amine groups *via* hydrogen bonded six-membered ring structures, tilted 'upward' and 'downward'. The effect of electronic (or electrostatic) interactions as well as of the internal hydrogen bonds on the experimentally observed interactivity of basic sites along the protonation processes were also demonstrated.

In order to get a clearer characterization of the protonation scheme of this molecule and an exact picture of its acid–base properties, we have calculated the protonation microconstants. These microscopic protonation constants were calculated as follows.

The complete protonation scheme of H_2L^1 can be seen in Scheme 1 which shows that as many as 32 microconstants can be derived for this ligand. Considering, however, the symmetry relations existing in this molecule, identical basicity can be assumed for twin donors (*e.g.* $k^{O} = k^{O'}$, $k^{N} = k^{N'}$, $k^{N}_{O} = k^{N'}_{O}$). On the other hand, it is known that protonation at one basic site modifies the basicities of other sites in the molecule. This modification can be quantified in terms of interactivity parameters ($\Delta\log k$).[19,20]

$$\Delta\log k_{x-y} = \log k^{x}_{y} - \log k^{x} = \log k^{y}_{x} - \log k^{y} \qquad (1)$$

Interactivity parameters are assumed to have two important properties: (*i*) they have identical values in the same moieties of different molecules and (*ii*) they are largely independent of the protonation stage of sites other than x and y. Thus, the value of the interactivity parameter can be transferred from one molecule to another, provided the moiety considered is the same. Taking the above principles together to quantify the acid–base properties of H_2L^1, one has to know independent microconstants and interactivity parameters. For this ligand, the various possibilities of interactivity are shown in Scheme 2.

From the analysis of the protonation and interactivity schemes for H_2L^1 (Schemes 1 and 2), one can conclude that in addition to the macroconstants, knowledge of the k^{O} and k^{N} microconstants and four independent interactivity parameters, $\Delta\log k_{N-N'}$, $\Delta\log k_{N-O}$, $\Delta\log k_{N-O'}$ and $\Delta\log k_{O-O'}$, are necessary for the adequate acid–base characterization of H_2L^1. Combining k^{O} and k^{N} microconstants plus the appropriate set of interactivity parameters, any microconstant can be obtained [*e.g.* eqns. (2) and (3)]

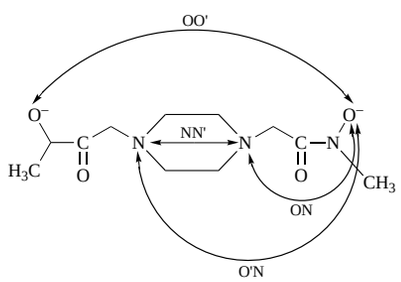

N, N'	$\Delta\log k_{N—N'} = \log k^{N} - \log k^{N}_{N'} = \log k^{N'} - \log k^{N'}_{N}$
N, O	$\Delta\log k_{N—O} = \log k^{N} - \log k^{N}_{O} = \log k^{O} - \log k^{O}_{N}$
	$= \log k^{N'} - \log k^{N'}_{O'} = \log k^{O'} - \log k^{O'}_{N}$
N, O'	$\Delta\log k_{N—O'} = \log k^{N} - \log k^{N}_{O'} = \log k^{O'} - \log k^{O'}_{N}$
	$= \log k^{N'} - \log k^{N'}_{O} = \log k^{O} - \log k^{O}_{N'}$
O, O'	$\Delta\log k_{O—O'} = \log k^{O} - \log k^{O}_{O'} = \log k^{O'} - \log k^{O'}_{O}$

Scheme 2 Possibilities of interactivities in H_2L^1

$$k^{N}_{O} = k^{N} \times 10^{\Delta\log k_{N\text{-}O}} \qquad (2)$$

$$k^{O'}_{N,N'} = k^{O} \times 10^{\Delta\log k_{N\text{-}O}} \times 10^{\Delta\log k_{N\text{-}O'}} \qquad (3)$$

The resulting relationships between the cumulative macroconstants (β values), the microconstants and interactivity parameters are shown in eqns. (4)–(7).

$$\beta_1 = k^{O} + k^{N} + k^{N'} + k^{O'} = 2k^{N} + 2k^{O} \qquad (4)$$

$$\beta_2 = k^{O}k^{N} \times 10^{\Delta\log k_{N\text{-}O}} + k^{O'}k^{N} \times 10^{\Delta\log k_{N\text{-}O'}} + k^{O}k^{O'} \times 10^{\Delta\log k_{O\text{-}O'}} + k^{N}k^{N'} \times 10^{\Delta\log k_{N\text{-}N'}} + k^{N}k^{O'} \times 10^{\Delta\log k_{N\text{-}O'}} + k^{N'}k^{O'} \times 10^{\Delta\log k_{N'\text{-}O'}} = 2k^{O}k^{N}(10^{\Delta\log k_{N\text{-}O}} + 10^{\Delta\log k_{N\text{-}O'}}) + (k^{N})^2 \times 10^{\Delta\log k_{N\text{-}N'}} + (k^{O})^2 \times 10^{\Delta\log k_{O\text{-}O'}} \qquad (5)$$

$$\beta_3 = k^{O}k^{N} \times 10^{\Delta\log k_{N\text{-}O}}k^{N} \times 10^{\Delta\log k_{N\text{-}N'}} \times 10^{\Delta\log k_{N\text{-}O'}} + k^{O}k^{N} \times 10^{\Delta\log k_{N\text{-}O}}k^{O} \times 10^{\Delta\log k_{N\text{-}O'}} \times 10^{\Delta\log k_{O\text{-}O'}} + k^{O'}k^{N'} \times 10^{\Delta\log k_{N\text{-}O}}k^{N} \times 10^{\Delta\log k_{N\text{-}N'}} \times 10^{\Delta\log k_{N\text{-}O'}} + k^{O'}k^{N'} \times 10^{\Delta\log k_{N\text{-}O}}k^{O} \times 10^{\Delta\log k_{O\text{-}O'}} \times 10^{\Delta\log k_{N\text{-}O'}} =$$

$$2k^{O}k^{2N} \times 10^{\Delta\log k_{N\text{-}O}} \times 10^{\Delta\log k_{N\text{-}O'}} \times 10^{\Delta\log k_{N\text{-}N'}} +$$
$$2k^{N}k^{2O} \times 10^{\Delta\log k_{N\text{-}O}} \times 10^{\Delta\log k_{N\text{-}O'}} \times 10^{\Delta\log k_{O\text{-}O'}} =$$
$$2k^{O}k^{N} \times 10^{\Delta\log k_{N\text{-}O}} \times 10^{\Delta\log k_{N\text{-}O'}}(k^{N} \times 10^{\Delta\log k_{N\text{-}N'}} + k^{O} \times 10^{\Delta\log k_{O\text{-}O'}}) \quad (6)$$

$$\beta_4 = k^{O}k^{N} \times 10^{\Delta\log k_{N\text{-}O}}k^{N} \times 10^{\Delta\log k_{N\text{-}O'}} \times 10^{\Delta\log k_{N\text{-}N'}} \times k^{O} \times 10^{\Delta\log k_{O\text{-}O'}} \times 10^{\Delta\log k_{N\text{-}O}} \times 10^{\Delta\log k_{N\text{-}O'}} =$$
$$(k^{O})^2(k^{N})^2 \times (10^{\Delta\log k_{N\text{-}O}})^2 \times (10^{\Delta\log k_{N\text{-}O}})^2 \times 10^{\Delta\log k_{O\text{-}O'}} \times 10^{\Delta\log k_{N\text{-}N'}} \quad (7)$$

The protonation macroconstants (β values) were reported in a previous paper.[5] Values of log β_1, log β_2, log β_3 and log β_4 at 25 °C and 0.1 M KNO_3 are 9.53, 17.99, 214.66 and 27.10, respectively. The estimations of the four interactivity parameters were based on values for model compounds available in the literature. For example, $\Delta\log k_{N\text{–}N'}$ was assumed to be the same in H_2L^1 as in piperazine, a symmetrical molecule with an analogous structural moiety and two binding sites for which this interactivity parameter is given by eqn. (8). The value

$$\Delta\log k_{N\text{–}N'} = \log K_1 - \log K_2 + 0.6 \quad (8)$$

obtained is *ca.* −3.7 to −4.0 depending on the conditions (ionic strength).[12]

Given the large number of bonds separating the two hydroxamate groups in H_2L^1, one might assume that no interaction exists between these two sites. This means that $\Delta\log k_{O\text{–}O'} = 0$. However the protonation constants of long-chain α–ω dicarboxylic acids (*e.g.* adipic, pimelic, azelaic)[12] indicate that log K_1 − log K_2 differs somewhat from 0.6 (being 0.73–0.8). Thus, a small interaction between the two hydroxamates may also occur in H_2L^1.

The $\Delta\log k_{N\text{–}O}$ value was obtained from the analog α-alaninehydroxamic acid.[15] The nitrogen and hydroxamate groups are separated by the same number of bonds in H_2L^1 and α-alaninehydroxamic acid. The $\Delta\log k_{O\text{–}N}$ value for the latter compound is −1.12 and −1.09 for I = 0.2 M (KCl) and I = 1.0 M (KCl), respectively.[15]

Finally, calculations for the best fit of macroconstants (less than 0.01 log unit difference for each of the calculated and experimental log β values), gave the following results.

$$\log k^{N} = 8.52, \qquad \log k^{O} = 9.10$$
$$\Delta\log k_{N\text{–}N'} = -3.70, \qquad \Delta\log k_{N\text{–}O} = -1.12$$
$$\Delta\log k_{N\text{–}O'} = -0.95, \qquad \Delta\log k_{O\text{–}O'} = -0.32$$

Hence, a first conclusion is that there is no great difference between the basicities of the hydroxamic moiety and the piperazine nitrogen. This result is in full agreement with that expected from model studies.[12,15]

Comparison of the calculated interactivity parameters with the corresponding estimated ones shows very good agreement in the case of $\Delta\log k_{N\text{–}N'}$ and $\Delta\log k_{N\text{–}O}$. However, both $\Delta\log k_{O\text{–}O'}$ and $\Delta\log k_{N\text{–}O'}$ are somewhat higher than expected. The value expected for $\Delta\log k_{O\text{–}O'}$ was based on data from single-chain model compounds (different dicarboxylic acids) and the value for $\Delta\log k_{N\text{–}O'}$ was also based on an estimation that took into consideration only the number of bonds separating the donors concerned. However, if we take into account that the central piperazine ring transmits the effects *via* two ethylene moieties, the difference may be accounted for. In effect, a significant difference exists between the corresponding interactivity parameters on the 'double connecting ethylene' piperazine and the 'single connecting ethylene' ethylenediamine (−3.8 and −2.2, respectively). This clearly shows that the effect is greatly increased by the 'two way' interaction manner. This may be the reason why somewhat higher $\Delta\log k_{N\text{–}O'}$ and $\Delta\log k_{O\text{–}O'}$ values were obtained for H_2L^1.

Table 4 Microscopic protonation constants of H_2L^1 in log units (for assignment of microconstants see Scheme 2)

$k^{N} = k^{N'} = 8.5$	$k^{O} = k^{O'} = 9.1$
$k^{N}_{O} = k^{N'}_{O'} = 7.4$	$k^{O}_{N} = k^{O'}_{N'} = 8.0$
$k^{N'}_{O} = k^{N}_{O'} = 7.6$	$k^{O'}_{N} = k^{O}_{N'} = 8.2$
$k^{O'}_{O} = k^{O}_{O'} = 8.8$	$k^{N'}_{N} = k^{N}_{N'} = 4.8$
$k^{O}_{NN'} = k^{O}_{N'N} = 7.0$	$k^{N}_{ON'} = k^{N'}_{NO'} = 3.7$
$k^{N'}_{ON} = k^{N}_{N'O'} = 3.9$	$k^{O'}_{ON} = k^{O}_{O'N'} = 7.8$
$k^{O'}_{ON'} = k^{N}_{NO'} = 7.7$	$k^{N}_{OO'} = k^{N}_{O'O} = 6.5$
$k^{N'}_{ONO'} = k^{N}_{ON'O'} = 2.8$	$k^{O'}_{NN'O} = k^{O}_{NN'O} = 6.7$

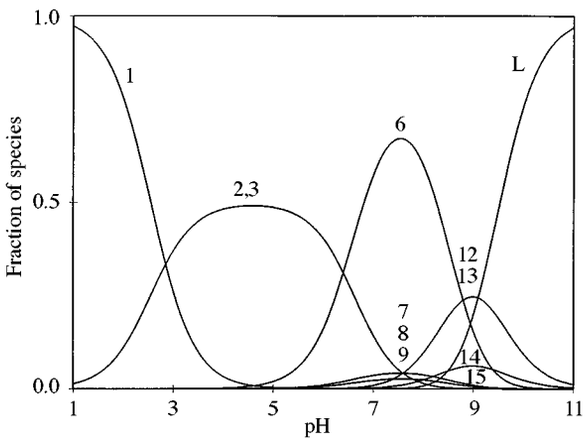

Fig. 5 Concentration distribution curves, calculated for individual species of H_2L^1 at different pH ($C_L = 2 \times 10^{-2}$ mol dm^{-3}). 1, H_4L^1; 2, $H_3L^1_{ONO'}$; 3, $H_3L^1_{ON'O}$; 4, $H_3L^1_{ONN'}$; 5, $H_3L^1_{NN'O'}$; 6, $H_2L^1_{OO'}$; 7, $H_2L^1_{NO'}$; 8, $H_2L^1_{N'O}$; 9, $H_2L^1_{ON}$; 10, $H_2L^1_{NN'}$; 11, $H_2L^1_{N'O}$; 12, HL^1_{O}; 13, $HL^1_{O'}$; 14, HL^1_{N}; 15, $HL^1_{N'}$.

Using the results above, all the values of the microconstants could be calculated and are listed in Table 4 (as logarithms). Based on the set of values presented in Table 4, microspeciation curves were obtained and are shown in Fig. 5. From the microconstant values one can conclude that the *N*-donors in this molecule are much less basic than the *O*-donors. With increasing pH, the protonated *N* moieties release most protons in the acid region, while deprotonation of an OH moiety starts only above pH 5.

Experimental

Reagents

All the hydroxamate ligands were prepared in our laboratory except the glycinehydroxamic acid, which is commercially available. All the reactions were monitored by TLC. Analytical reagents were used as supplied. The solvents were dried according to standard methods.[21] All reaction products were characterized by the usual methods of analysis: mp, IR, NMR and mass spectra.

Synthesis

The synthesis of the ligand H_2L^1 involved the previous preparation of *N*-methylchloroacetohydroxamic acid (HL^2) which was then used for *N*-substitution of the corresponding cyclic diamine, piperazine (L^5), in an alkaline medium, according to a method described in the literature.[5] The synthesis of the model piperidino(*N*-methylacetohydroxamic acid) (HL^4) employs a multi-step approach whereby an *O*-protected hydroxamic acid, *N*-methyl-*O*-benzylchloroacetohydroxamic acid, is synthesized by acyl condensation with *N*-methyl-*O*-benzylhydroxylamine which is achieved using previously reported methods.[4,22] The hydroxamic acid is then coupled with piperidine, followed by *O*-deprotection as the final step.

***N*-Methyl-*O*-benzylchloroacetohydroxamic acid.** A suspension of *N*-methyl-*O*-benzylhydroxylamine (1.55 g, 8.9 mmol) in tetrahydrofuran (75 ml) was cooled in an ice bath and potas-

sium carbonate (2.46 g, 17.8 mmol) was added and left stirring under N_2 for 0.5 h. Chloroacetyl chloride (1.05 g, 9.3 mmol) was dissolved in the same solvent (10 ml), added dropwise to the reaction mixture and stirred. After 6 h the reaction was finished, the reaction mixture was filtered and the filtrate evaporated under reduced pressure. The oil residue was dissolved in ethyl acetate (100 ml) and this solution was washed with water (50 ml), 0.5 M citric acid (2 × 50 ml), 0.6 M sodium bicarbonate (2 × 50 ml) and brine (50 ml). The organic extract was dried over Na_2SO_4 and evaporated *in vacuo* to give the hydroxamic acid as a colorless oil in 79% yield (1.501 g, 7.0 mmol). ν(neat)/cm^{-1} (C=O); $\delta_H(CDCl_3)$ 3.27 (s, 3H, CH_3), 4.12 (s, 2H, CH_2Cl), 4.89 (s, 2H, $ArCH_2$), 7.41 (m, 5H, ArH); (Anal. Calc. for $C_{10}H_{12}NO_2Cl$: C, 56.21; H, 5.62, N, 6.56%. Found: C, 56.59; H, 5.83; N, 6.95%).

Piperidino(*N*-methyl-*O*-benzylacetohydroxamic acid). A solution of piperidine (0.24 ml, 2.4 mmol) in dry dimethylformamide (30 ml) was cooled in an ice bath under N_2. Sodium hydride (0.06 g, 2.6 mmol) was then added and the mixture stirred. After 15 min, a solution of *N*-methyl-*O*-benzylchloroacetohydroxamic acid (0.51 g, 2.4 mmol) in the same solvent (10 ml) was added dropwise and the mixture was stirred for 7 h at room temperature. The reaction mixture was extracted in ethyl acetate (80 ml) and washed with brine (3 × 50 ml). The organic extract was dried over Na_2SO_4 and the solvent was evaporated under reduced pressure to give the reaction product as an oil in 75% yield (0.47 g; 1.8 mmol). ν(neat)/cm^{-1} 1660; $\delta_H(CDCl_3)$ 1.60 (m, 6H, NCH_2CH_2 CH_2CH_2), 2.47 (m, 4H, NCH_2), 3.21 (s, 3H, CH_3), 3.23 (s, 2H, CH_2CO), 4.89 (s, 2H, $ArCH_2$), 7.41 (m, 5H, ArH).

Piperidino(*N*-methylacetohydroxamic acid), HL[4]. A solution of piperidino(*N*-methyl-*O*-benzylacetohydroxamic acid) (0.46 g, 1.8 mmol) in methanol (30 ml) was treated with Pd on carbon (10%, 0.15 g) under H_2 (1 atm) and the mixture was stirred for 4 h at room temperature. The reaction mixture was filtered and the solvent was evaporated. The residue was then chromatographed on a silica gel column, using methanol–dichloromethane (2:5) as eluent. The desired product was collected and recrystallized from ethanol–diethyl ether to yield the final product as white crystals (157 mg, 51%); mp 86–88 °C. ν(KBr)/cm^{-1} 1650 (C=O); $\delta_H(D_2O$; pD = 8.58) 1.64 (m, 2H, $NCH_2CH_2CH_2$), 1.86 (m, 4H, NCH_2CH_2), 3.21 (m, 7H, NCH_3 + NCH_2), 3.97 (s, 2H, CH_2CO); *m*/*z* 172 [M^+], 170 [M − 2H]$^+$, 155 [M − OH]$^+$; (Anal. Calc. for $C_8H_{16}N_2O_2$·0.5HCl: C, 50.46; H, 8.67; N, 14.72%. Found: C, 50.51; H, 8.98; N, 14.34%).

NMR measurements

The dissociation macroconstants were determined by potentiometric titrations as described previously.[5] The ^{1}H NMR spectra were recorded on a Varian Unity 300 spectrometer at 25 °C. Solutions of the ligands (2×10^{-2} mol dm^{-3}) for NMR pH titrations were made in D_2O with sodium 3-(trimethylsilyl)-[2,2,3,3-$^2H_4$]propionate as reference. The pD* of the solution (operational pD, since the pH meter was standardized with conventional buffers at pH 4 and 7) was adjusted with DCl and KOD, and was measured with a 420A Orion pH meter, equipped with a combined Ingold U402-M3-S7/200 microelectrode.

Calculation of microconstants

Microconstants and interactivity parameters were calculated by using the 'Scientist' non-linear curve-fitting software adjusted to the relationships in eqns. (4)–(7).

Molecular modeling simulations

To perform the molecular modeling of H_2L^1, HL^4 and related species, we started with both the most stable cyclic backbone conformations, chair and twist-boat, for piperazine (L^5) and piperidine (L^6), as derived by Burkert and Allinger[23] for six-membered rings. The minimum energy geometries corresponding to the *N*-substituted compounds were then located by molecular dynamics/molecular mechanics (MD/MM) methods, using the BIOSYM program.[24] A final refinement with full geometry optimization was then carried out, employing the PRECISE option of the AM1 semi-empirical SCF-Method, included in the MOPAC program that is contained in the same package of software. The AM1 method was chosen because it is thought to provide an adequate description of hydrogen bonded conformations.[25] Although our AM1 calculations neglect solvation effects on the hydrogen bond interactions, some compensation of this effect was taken into account in the final MM/AM1 calculations *via* the distance dependence option for the electrostatic interactions ($E_{elec} = \Sigma\, q_i q_j / \varepsilon\, q_{ij}$, summed over all pairs of *i* and *j* atoms, where q_i and q_j are the charges on individual atoms within each pair and r_{ij} is the distance between them).

Acknowledgements

The authors thank the Junta Nacional de Investigação Científica (JNICT) for financial assistance: B. N. for the grant OTKA T 175070; E. F. for grant OTKA T 023612.

References

1 B. F. Matzanke, G. Mueller and K. N. Raymond, in *Iron Carriers and Iron Proteins*, ed. T. M. Loehr, VCH, New York, 1989, ch. 1; K. N. Raymond, *Pure Appl. Chem.*, 1994, **66**, 773.
2 A. L. Crumblis, in *Handbook of Microbial Iron Chelates*, ed. G. Winkelmann, CRC Press, Boca Raton, FL, 1991, ch. 7.
3 M. A. Santos, M. A. Esteves, M. C. T. Vaz and M. L. S. Gonçalves, *Inorg. Chim. Acta*, 1993, **214**, 47.
4 M. A. Esteves, M. C. T. Vaz, M. L. S. Gonçalves, E. Farkas and M. A. Santos, *J. Chem. Soc., Dalton Trans.*, 1995, 2565.
5 M. A. Santos, M. A. Esteves, M. C. T. Vaz and M. L. S. Gonçalves, *J. Chem. Soc., Dalton Trans.*, 1993, 927.
6 M. A. Santos, M. A. Esteves and J. M. G. Martinho, *J. Chem. Soc., Dalton Trans.*, 1993, 3123.
7 C. J. Carrano and K. N. Raymond, *J. Am. Chem. Soc.*, 1978, **100**, 5371.
8 J. R. Ascenso, M. A. Santos, J. J. R. Fraústo da Silva, M. Cândida, M. C. T. Vaz and M. G. B. Drew, *J. Chem. Soc., Perkin Trans. 2*, 1990, 2215.
9 T. L. Sayer and D. L. Rabenstein, *Can. J. Chem.*, 1976, **54**, 3392.
10 B. Kurzak, H. Kozlowski and E. Farkas, *Coord. Chem. Rev.*, 1992, **114**, 169.
11 H. Irving and L. D. Pettit, *J. Chem. Soc.*, 1963, 3051.
12 A. E. Martell and R. M. Smith, *Critical Stability Constants*, Plenum Press, New York, 1975, vol. 6.
13 J. L. Sudmeier and C. N. Reilley, *Anal. Chem.*, 1964, **36**, 1699; 1707.
14 J. F. Desreux, E. Merciny and M. F. Loncin, *Inorg. Chem.*, 1981, **20**, 987.
15 E. Farkas, T. Kiss and B. Kurzak, *J. Chem. Soc., Perkin Trans. 2*, 1990, 1255.
16 M. A. Santos, A. M. Lobo and S. Prabhakar, *Rev. Port. Quím.*, 1989, **31**, 48.
17 J. Rodrigues, *J. Comput. Chem.*, 1994, **15**, 183.
18 B. H. Besler, K. M. Merz and P. Roldman, *J. Comput. Chem.*, 1990, **11**, 431.
19 B. Noszál, in *Biocoordination Chemistry*, ed. K. Burger, Ellis Horwood, New York, 1990, p. 18.
20 B. Noszál and R. Kassai-Táncsos, *Talanta*, 1991, **38**, 1439.
21 P. D. Perrin, W. L. F. Armarego and D. R. Perrin, *Purification of Laboratory Chemicals*, Pergamon Press, London, 1965.
22 B. H. Lee, G. F. Gerfen and M. J. Miller, *J. Org. Chem.*, 1984, **49**, 248.
23 U. Burkert and N. L. Allinger, ACS Monograph 177, Washington DC, 1982.
24 INSIGHT/DISCOVER: Insight II, version 95.0, Biosym Inc., San Diego, CA, 1995.
25 M. J. S. Dewar, E. G. Zoebisch, E. F. Healy and J. J. P. Stewart, *J. Am. Chem. Soc.*, 1985, **107**, 3902.

Paper 7/02138K
Received 23*rd February* 1997
Accepted 29*th May* 1997